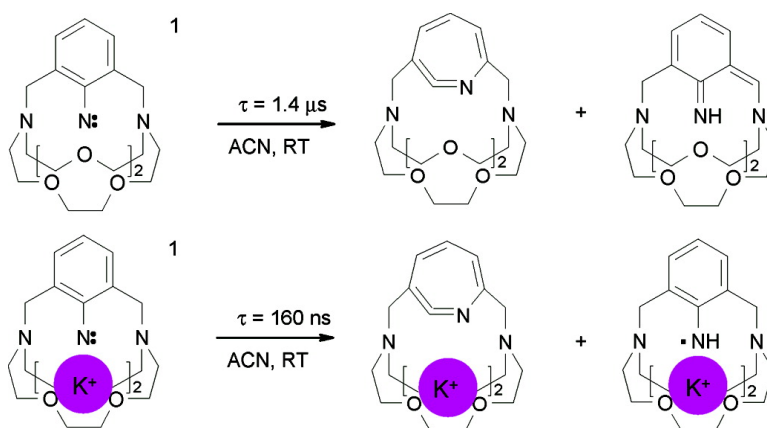


Photochemistry of an Azido-Functionalized Cryptand: Controlling the Reactivity of an Extremely Long-Lived Singlet Aryl Nitrene by Complexation to Alkali Cations

Qtz Bucher, Christina Tnshoff, and Athanassios Nicolaidis

J. Am. Chem. Soc., **2005**, 127 (18), 6883-6892 • DOI: 10.1021/ja0447208 • Publication Date (Web): 16 April 2005

Downloaded from <http://pubs.acs.org> on March 25, 2009



More About This Article

Additional resources and features associated with this article are available within the HTML version:

- Supporting Information
- Links to the 1 articles that cite this article, as of the time of this article download
- Access to high resolution figures
- Links to articles and content related to this article
- Copyright permission to reproduce figures and/or text from this article

[View the Full Text HTML](#)

Photochemistry of an Azido-Functionalized Cryptand: Controlling the Reactivity of an Extremely Long-Lived Singlet Aryl Nitrene by Complexation to Alkali Cations

Götz Bucher,^{*,†} Christina Tönshoff,[†] and Athanassios Nicolaides[‡]

Contribution from the Lehrstuhl für Organische Chemie II, Ruhr-Universität Bochum, Universitätsstrasse 150, 44801 Bochum, Germany, and Department of Chemistry, University of Cyprus, P.O. Box 20537, 1678 Nicosia, Cyprus

Received September 1, 2004; E-mail: goetz.bucher@rub.de

Abstract: Photolysis of the cryptand **1**, bearing an intraannular azido substituent, results in a complex photochemistry. Low-temperature photolysis yields the triplet nitrene ³**2**, which has been characterized by EPR spectroscopy. Small differences in ZFS parameters are detected between the uncomplexed nitrene-functionalized ligand (in EtOH: $D' = 0.93 \text{ cm}^{-1}$) and its sodium (NaBr@³**2** in EtOH: $D' = 0.88 \text{ cm}^{-1}$) and potassium (KBr@³**2** in MTHF: $D' = 0.89 \text{ cm}^{-1}$) complexes. If the photolysis of the free ligand is conducted at ambient temperature, a derivative of *o*-aminobenzaldehyde **4** is found to be the main product, which is formed by reaction of the *o*-iminoquinone methide **9** with water. The latter can be detected by UV/vis spectroscopy. Its lifetime is $\tau = 254 \text{ s}$ in acetonitrile solution at ambient temperature. In the presence of diethylamine, the methyleneazepine derivative **5** is formed, which is indicative of didehydroazepine formation (**7**). Room-temperature photolysis of acetonitrile solutions of the sodium or potassium complexes also results in formation of the *o*-aminobenzaldehyde derivative. In the presence of diethylamine, however, no methyleneazepine **5** is found. Formation of the aniline derivative **8** instead points to free radical processes. Laser flash photolysis (LFP) of acetonitrile solutions of **1** leads to the detection of a short-lived ($\tau = 1.4 \mu\text{s}$, $\lambda_{\text{max}} = 445 \text{ nm}$ plus weak absorption at $\lambda > 500 \text{ nm}$) intermediate **A**, which decays to transient **B** ($\tau = 8 \text{ ms}$, $\lambda_{\text{max}} = 295$ and ca. $350\text{--}400 \text{ nm}$). LFP of acetonitrile solutions of complexes NaBr@**1** and KBr@**1** gives similar transient spectra. In the presence of sodium and potassium cations, the lifetime of the short-lived transient **A** is reduced (Na⁺: **A'**, $\tau = 200 \text{ ns}$; K⁺: **A''**, $\tau = 160 \text{ ns}$). Transients **A'** and **A''** decay to long-lived transients **B' + C'** (**B'' + C''**). Based on the results of our product studies, a comparison with the low-temperature results, and quantum mechanical calculations, the transients **A**, **A'**, and **A''** are identified as singlet nitrenes ¹**2**, NaBr@¹**2**, and KBr@¹**2**, while the long-lived transients **B**, **B'**, and **B''** are assigned to didehydroazepines **7**, NaBr@**7**, and KBr@**7**. Transients **C'** and **C''** can be assigned to aminyl radicals NaBr@**16** and KBr@**16**.

Introduction

Nitrenes are electron-deficient diradicals with a formal electron sextet at the nitrogen atom. Photolysis or thermolysis of aryl azides initially yields singlet aryl nitrenes, which, depending on factors such as temperature and substitution, either undergo intersystem crossing to the triplet ground state or rearrange to didehydroazepines via bicyclic azirines.^{1–5} Triplet

nitrenes also are strongly electrophilic reactive intermediates, which typically decay by dimerization to azo dyes or via intermolecular hydrogen abstraction.^{6–8} Due to the lone pair at the nitrene center, nitrenes can in principle also serve as nucleophiles. Thus, generation of singlet aryl nitrenes in acidic media leads to extremely rapid N-protonation, resulting in the formation of nitrenium ions.^{9,10} The lone pair at the electron-deficient nitrene center represents a hard nucleophile. Therefore, it does not play a role in reactions with soft electrophiles. Fluorine atoms, whose lone pairs also show a very small polarizability and are energetically very low-lying, can be complexed to alkali or alkaline earth cations, if they are placed

[†] Ruhr-Universität Bochum.

[‡] University of Cyprus.

(1) Platz, M. S. *Acc. Chem. Res.* **1995**, *28*, 487.

(2) Schuster, G. B.; Platz, M. S. In *Advances in Photochemistry*; D. H. Volman, G. Hammond, D. C. Neckers, Eds.; John Wiley & Sons: New York, 1992; pp 69–143.

(3) (a) Bucher, G. Photochemical Reactivity of Azides. In *CRC Handbook of Photochemistry*, 2nd ed.; CRC Press: Boca Raton, 2003; Chapter 44. (b) Platz, M. S. Nitrenes. In *Reactive Intermediate Chemistry*; Wiley-Interscience: Hoboken, 2004; Chapter 11. (c) Doyle, M. P. Synthetic Carbene and Nitrene Chemistry. In *Reactive Intermediate Chemistry*; Wiley-Interscience: Hoboken, 2004; Chapter 12. (d) Tokitoh, N.; Saiki, T.; Okazaki, R. *Chem. Commun.* **1995**, 1899.

(4) Gritsan, N. P.; Yuzawa, T.; Platz, M. S. *J. Am. Chem. Soc.* **1997**, *119*, 5059.

(5) Born, R.; Burda, C.; Senn, P.; Wirz, J. *J. Am. Chem. Soc.* **1997**, *119*, 5061.

(6) Leyva, E.; Platz, M. S.; Perys, G.; Wirz, J. *J. Am. Chem. Soc.* **1986**, *108*, 3783.

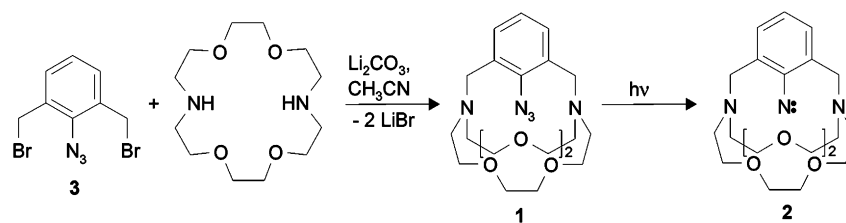
(7) Hayes, J. C.; Sheridan, R. S. *J. Am. Chem. Soc.* **1990**, *112*, 5879.

(8) Bucher, G.; Scaiano, J. C.; Sinta, R.; Barclay, G.; Cameron, J. *J. Am. Chem. Soc.* **1995**, *117*, 3848.

(9) McClelland, R. A.; Davidse, P. A.; Hadzialic, G. *J. Am. Chem. Soc.* **1995**, *117*, 4173.

(10) McClelland, R. A.; Kahley, M. J.; Davidse, A.; Hadzialic, G. *J. Am. Chem. Soc.* **1996**, *118*, 4794.

Scheme 1



as intraannular substituents in crown ethers or cryptands.^{11,12} In terms of both structure and electrostatic interaction between intraannular substituent and alkali cation, nitrene-substituted cryptands such as **2** (Scheme 1) and intraannularly fluorine-substituted cryptands thus are alike. This makes it conceivable that the nitrene center in **2** could indeed function as coordinating site for metal ions. Our motivation for investigating the photochemistry of azido-functionalized cryptand **1** and some of its complexes was threefold. First, unlike transition metal–nitrene (imido) complexes,^{3c} complexes of aryl nitrenes or didehydroazepines and alkali cations are virtually unexplored, and it was a priori completely unclear whether complexation would result in stabilization or destabilization of the reactive intermediates involved. Second, the unusual electron-rich environment of nitrene **2** could have interesting consequences on its reactivity (resulting, for example, in intramolecular ylide formation), even in the absence of added alkali cations. That unusual nitrene reactivity may indeed be induced by such an environment has become evident by a study on calixarene-functionalized aryl nitrenes by Okazaki and co-workers, who observed nitrene cycloaddition to a benzene ring not directly connected with the nitrene center.^{3d} Third, the cryptand system represents a sterically rather demanding substituent. Steric shielding of the reactive center of secondary reaction intermediates, such as didehydroazepines, could result in their stabilization. The characterization of nitrene **2** thus constitutes a challenging and rewarding problem, which may well serve to extend our knowledge of nitrene chemistry in particular and reactive intermediate chemistry in general.

Experimental and Theoretical Methods

The synthesis of **1**, $\text{NaBr}@\mathbf{1}$, and $\text{KBr}@\mathbf{1}$ was achieved by reacting diaza-18-crown-6 with 2,6-bis(bromomethyl)azidobenzene **3** in the presence of lithium carbonate (free ligand) or sodium or potassium carbonate (complexes) (Scheme 1). It is described in detail elsewhere.¹³

Preparative Irradiations. A 50 mg sample of the cryptand is added to a quartz vessel, which is sealed with a septum. The compound is dissolved in 30 mL of CH_3CN (HPLC-grade). In quenching experiments, the quencher is added via syringe (0.075 mL of H_2O , corresponding to 0.25%; or 2.5 mL of Et_2NH , corresponding to 8%). The solution is purged with Ar for 30 min and then irradiated for 45 min at $\lambda \geq 320$ nm. After removal of the solvent, the residue is taken up in CH_2Cl_2 . The products are isolated via column chromatography (basic alumina; $\text{CH}_2\text{Cl}_2/\text{MeOH}$ and silica gel; *tert*-butyl methyl ether/ Et_2NH).

Characterization of Aldehyde 4. ^1H NMR (400 MHz, CD_2Cl_2): δ 2.03 (s, br, 2 H), 2.47 (s, 2 H), 2.76 (tr, 4 H), 3.01 (tr, 4 H), 3.47–3.50 (m, 4 H), 3.53–3.59 (m, 12 H), 6.76 (tr, 1 H), 7.20 (d, 1 H), 7.33 (d, 1 H), 8.32 (s, br, 1 H), 9.93 (s, 1 H). ^{13}C NMR (100 MHz, CD_2Cl_2):

δ 21.14, 49.89, 58.83, 68.73, 70.48, 70.76 (two resonances), 118.30, 121.52, 127.14, 133.03, 138.05, 150.46, 194.31. IR (film): $\tilde{\nu}$ 3471 (m), 2877 (s), 1661 (vs), 1517 (m), 1471 (s), 1384 (s), 1352 (s), 1299 (m), 1247 (s), 1211 (s), 1116 (vs), 969 (m), 832 (m), 770 (m) cm^{-1} . UV/vis (6.22×10^{-4} M in CH_3CN): λ_{max} 370 nm (ϵ 2100 $\text{dm}^3 \text{mol}^{-1} \text{cm}^{-1}$). MS (EI): m/z (%) 395 (58, M^+), 337 (5, $\text{M}^+ - \text{NCH}_2\text{CH}_2\text{O}$), 292 (12, $\text{M}^+ - \text{NC}_4\text{H}_7\text{O}$), 279 (8), 261 (100, $\text{N}_2\text{C}_{12}\text{H}_{25}\text{O}_4$), 236 (5), 220 (5), 187 (5), 174 (15), 148 (10), 134 (60, $\text{M}^+ - \text{N}_2\text{C}_{12}\text{H}_{25}\text{O}_4$), 118 (18), 100 (30), 86 (25), 79 (15), 70 (22), 56 (85), 43 (30).

Characterization of Methylene Azepine 5. ^1H NMR (CD_2Cl_2 , 400 MHz): δ 1.06 (tr, 6 H), 2.78–2.80 (m, 4 H), 2.82–2.85 (m, 4 H), 3.36–3.40 (m, 6 H), 3.57–3.60 (m, 16 H), 4.84 (s, 1 H), 4.86 (s, 1 H), 5.62 (d, 1 H), 5.72 (d, 1 H), 6.12–6.16 (dd, 1 H). ^{13}C NMR (CD_2Cl_2 , 400 MHz): δ 12.77, 42.50 (br), 49.21, 53.79, 70.02, 70.20, 70.73 (two resonances), 107.69, 112.32, 117.35, 129.61, 136.92, 147.72, 150.53. IR (film): $\tilde{\nu}$ 3410 (s), 2872 (s), 1677 (m), 1642 (m), 1626 (m), 1589 (m), 1562 (m), 1521 (m), 1454 (m), 1355 (m), 1294 (m), 1116 (s) cm^{-1} . MS (EI): m/z (%): 450 (100, M^+), 421 (10, $\text{M}^+ - \text{C}_2\text{H}_5$), 389 (10), 175 (5), 275 (10), 261 (22, $\text{C}_{12}\text{H}_{25}\text{N}_2\text{O}_4$), 230 (15), 203 (15), 190 (70, $\text{C}_{12}\text{H}_{18}\text{N}_2$), 175 (35), 161 (20), 145 (18), 132 (65), 118 (60), 91 (40), 72 (38), 56 (85).

Characterization of Aniline Derivative 8. Mp: 138 °C. ^1H NMR (CDCl_3 , 400 MHz): δ 2.68–2.74 (m, 4 H), 2.81–2.87 (m, 4 H), 3.34–3.38 (m, 4 H), 3.41–3.43 (m, 4 H), 3.46–3.51 (m, 4 H), 3.56–3.61 (m, 4 H), 3.65 (s, 4 H), 6.49 (tr, 1 H), 6.86 (d, 2 H). ^{13}C NMR (CDCl_3 , 100 MHz): δ 57.34, 60.92, 69.41, 70.53, 115.35, 125.31, 127.99, 149.54. IR (KBr): $\tilde{\nu}$ 3393 (vs), 3341 (s), 2905 (m), 2855 (s), 2794 (s), 1643 (m), 1597 (m), 1468 (s), 1396 (m), 1373 (m), 1354 (s), 1344 (s), 1304 (m), 1279 (m), 1256 (m), 1164 (m), 1113 (vs), 1071 (s), 1056 (s), 1034 (m), 1019 (m), 999 (m), 986 (m), 943 (m), 932 (m), 921 (m), 865 (m), 827 (m), 785 (m), 765 (s), 737 (m) cm^{-1} . MS (EI): m/z (%) 379 (85, M^+), 364 (85, $\text{M}^+ - \text{NH}$), 334 (10), 304 (20), 290 (15), 276 (30), 261 (25, $\text{C}_{12}\text{H}_{25}\text{N}_2\text{O}_4^+$), 247 (10), 235 (15), 222 (5), 205 (5), 187 (15), 159 (22), 132 (55), 118 (100, $\text{C}_8\text{H}_8\text{N}^+$), 100 (20), 91 (50), 56 (65). $\text{C}_{20}\text{H}_{33}\text{N}_3\text{O}_4$ (379.5): calcd C 63.29, H 8.76, N 11.07; found C 63.25, H 8.73, N 10.58.

Low-Temperature Spectroscopy. X-band EPR spectra were recorded with a Bruker Elexsys E500 EPR spectrometer with an ER077R magnet (75 mm pole cap distance) and an ER047 XG-T microwave bridge. Solutions (ca. 1 mM) of **1** and its complexes in ethanol or 2-methyltetrahydrofuran (MTHF) were cooled to $T = 5$ K using a Bruker ESR-900 liquid helium cryostat with an Oxford Instruments ITC 503 temperature controller. They were photolyzed using the output of a Hg high-pressure lamp (Oriol).

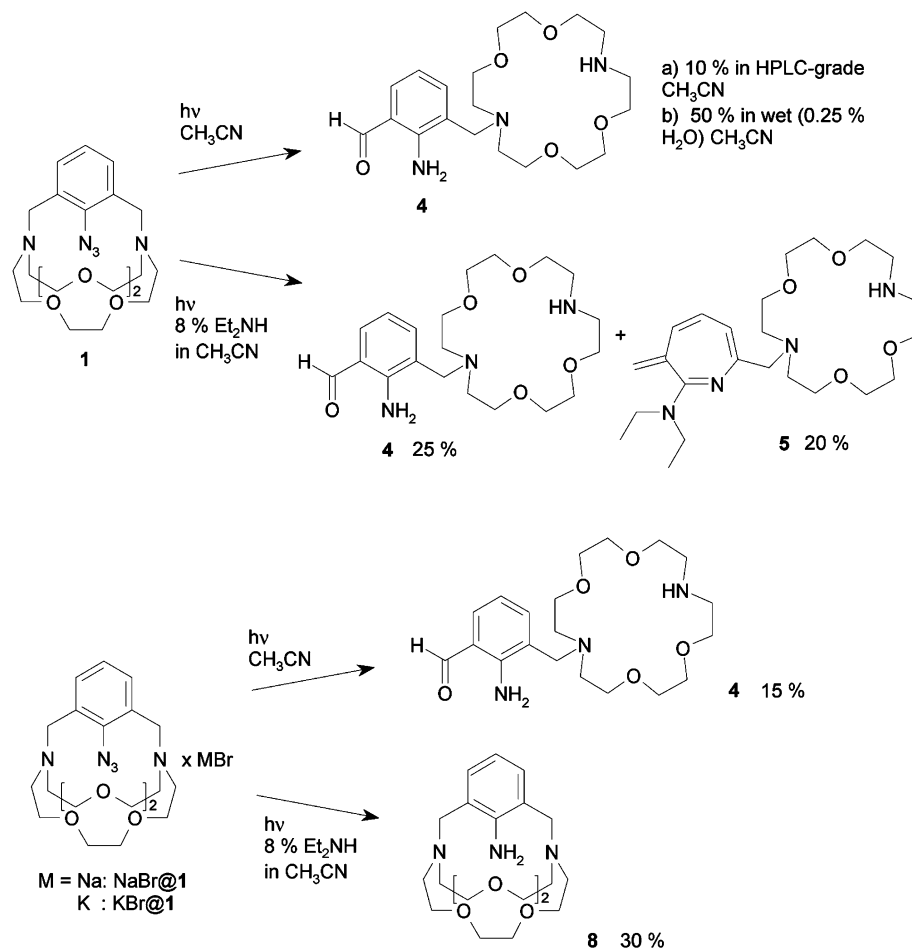
Low-Temperature UV/Vis Experiments. A solution of the azide in an appropriate spectroscopic grade solvent or solvent mixture (**1** in EPA or MTHF, $\text{NaBr}@\mathbf{1}$ and $\text{KBr}@\mathbf{1}$ in EPA, ca. 0.2 mM) in a quartz cell (optical path length 1 cm) was degassed by three freeze–pump–thaw cycles and placed in an Oxford DN 1704 liquid nitrogen cryostat with an ITC4 temperature controller. The temperature was set to 77 K. The sample was irradiated by means of a 500 W high-pressure mercury lamp (Oriol). Wavelength selection was achieved by the use of dichroic mirrors (Oriol, 260–300 nm or 350–450 nm) and cutoff filters (Schott). UV/vis spectra were recorded on a Hewlett-Packard 8452A diode array spectrometer.

(11) Plenio, H.; Diodone, R. *Angew. Chem.* **1994**, *106*, 2267; *Angew. Chem., Int. Ed.* **1994**, *33*, 2175.

(12) Plenio, H.; Diodone, R. *J. Am. Chem. Soc.* **1996**, *118*, 356.

(13) Tönshoff, C.; Merz, K.; Bucher, G. *Org. Biomol. Chem.* **2005**, *303*.

Scheme 2



Laser Flash Photolysis. The system employed has already been described.¹⁴ The azidocryptands were excited using the fourth harmonic ($\lambda = 266$ nm) of a Nd:YAG laser (Quanta-Ray Lab 130, 50 mJ/pulse, 7 ns pulse duration). The concentration of **1** was 6.4×10^{-5} M in acetonitrile (NaBr@**1**: 2.6×10^{-4} M; KBr@**1**: 2.2×10^{-4} M). A flow cell was used in order to avoid buildup of photoproducts. Prior to experiments, the solutions were purged with argon for ca. 20 min.

Calculations. The program package Gaussian 98¹⁵ was used for the DFT calculations. All calculated minima and transition states were characterized as such by performing a vibrational analysis. All calculated reaction and activation enthalpies include a zero-point vibrational energy correction. MCSCF (CASSCF) calculations were performed using the GAMESS software package.¹⁶ The active space consisted of eight electrons and eight MOs (the six π orbitals of the benzene carbons and one π and one σ orbital of the nitrene center). The STO-3G basis set (for a total of 166 basis functions) was used for these computations.

Results and Discussion

Product Studies. The photochemistry of **1**, NaBr@**1**, and KBr@**1** was investigated by product analysis. Chromatographic workup of the photolyzate yielded the products shown in Scheme 2:

The formation of the 2-aminobenzaldehyde derivative **4** can be rationalized to be occurring via iminoquinone methide **9** as intermediate, which reacts with water to **4** via intermediate **10** (Scheme 3). It is worthwhile mentioning that even in relatively dry, spectroscopically pure acetonitrile, **4** is formed in significant yield. This points to a long lifetime of **9**. In the presence of 8% diethylamine, the formation of methyleneazepine **5**^{17–19} is observed in addition to the formation of **4**. Product **5** is probably formed by addition of diethylamine to didehydroazepine **7**, followed by elimination of the diaza-18-crown-6 ring (Scheme 3). Photolysis of the sodium or potassium bromide complexes NaBr@**1**/KBr@**1** in acetonitrile leads to a similar product mixture (Scheme 1). The formation of aniline derivative **8** in the presence of diethylamine, however, needs to be pointed out. It is indicative of free radical nitrene reactivity (H-abstraction from HNet₂), for which there is no evidence in the case of the uncomplexed cryptand.

If a solution of **1** (1 mmol in CH₃CN) is briefly irradiated at ambient temperature (3 min, $\lambda > 320$ nm), a red solution is

(14) Bucher, G. *Eur. J. Org. Chem.* **2001**, 2463.

(15) Frisch, M. J.; Trucks, G. W.; Schlegel, H. B.; Scuseria, G. E.; Robb, M. A.; Cheeseman, J. R.; Zakrzewski, V. G.; Montgomery, J. A., Jr.; Stratmann, R. E.; Burant, J. C.; Dapprich, S.; Millam, J. M.; Daniels, A. D.; Kudin, K. N.; Strain, M. C.; Farkas, O.; Tomasi, J.; Barone, V.; Cossi, M.; Cammi, R.; Mennucci, B.; Pomelli, C.; Adamo, C.; Clifford, S.; Ochterski, J.; Petersson, G. A.; Ayala, P. Y.; Cui, Q.; Morokuma, K.; Malick, D. K.; Rabuck, A. D.; Raghavachari, K.; Foresman, J. B.; Cioslowski, J.; Ortiz, J. V.; Baboul, A. G.; Stefanov, B. B.; Liu, G.; Liashenko, A.; Piskorz, P.; Komaromi, I.; Gomperts, R.; Martin, R. L.; Fox, D. J.; Keith, T.; Al-Laham, M. A.; Peng, C. Y.; Nanayakkara, A.; Gonzalez, C.; Challacombe, M.; Gill, P. M. W.; Johnson, B.; Chen, W.; Wong, M. W.; Andres, J. L.; Gonzalez, C.; Head-Gordon, M.; Replogle, E. S.; Pople, J. A. *Gaussian 98*, Revision A.9; Gaussian, Inc.: Pittsburgh, PA, 1998.

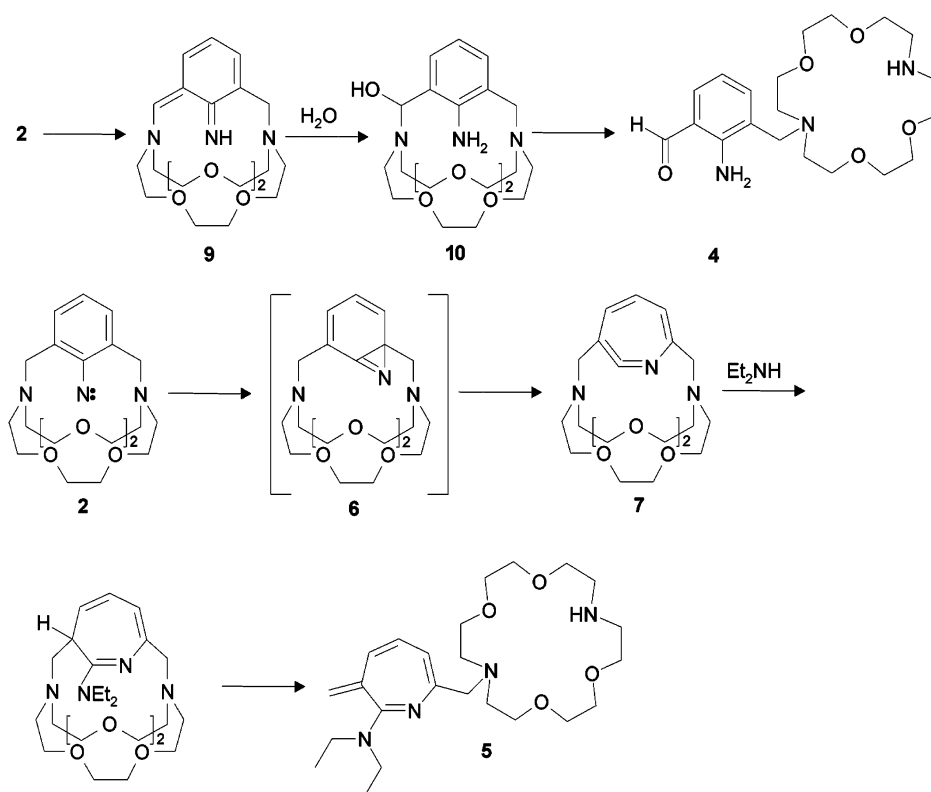
(16) Schmidt, M. W.; Baldrige, K. K.; Boats, J. A.; Elbert, S. T.; Gordon, M. S.; Jensen, J. H.; Koseki, S.; Matsunaga, N.; Nguyen, K. A.; Su, S.; Windus, T. L.; Dupuis, M.; Montgomery, J. A., Jr. *J. Comput. Chem.* **1993**, *14*, 1347.

(17) Bucher, G. *Angew. Chem.* **1999**, *111*, 1247; *Angew. Chem., Int. Ed.* **1999**, *38*, 1192.

(18) DeGraff, B. A.; Gillespie, D. W.; Sundberg, R. J. *J. Am. Chem. Soc.* **1974**, *96*, 7491.

(19) Bucher, G. *Eur. J. Org. Chem.* **2001**, 2447.

Scheme 3



obtained. The UV/vis spectrum of this solution shows absorption bands at $\lambda_{\text{max}} = 470$ nm (broad) and around $\lambda = 350$ nm (Figure 1). The red color disappears upon letting the solution stand for a couple of minutes. The decay rate constant was determined by UV/vis spectroscopy as $k = 3.93 \times 10^{-3} \text{ s}^{-1}$, which corresponds to a lifetime of $\tau = 254$ s (measured at $\lambda = 476$ nm). Adding a small amount of water via syringe leads to spontaneous discoloration, whereas addition of acrylonitrile does not result in a reaction. On the basis of the similarity of its UV/vis spectrum to the UV/vis spectra of other iminoquinone methides^{14,19} the red product is identified as iminoquinone methide **9** (configuration (*Z/E*) around the $\text{C}=\text{N}$ bond unknown). The activation enthalpy for the Diels–Alder reaction of *Z*-**9**

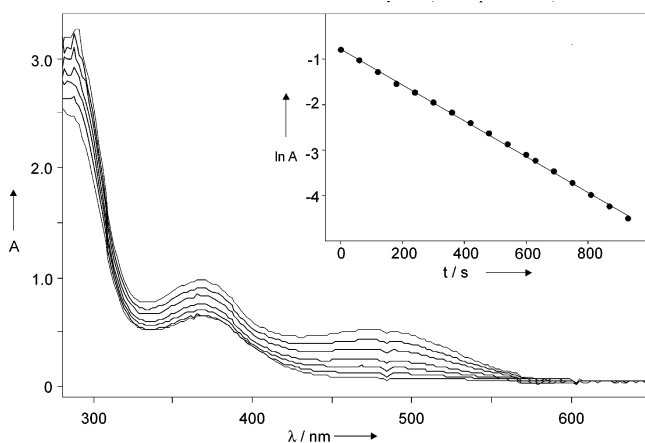


Figure 1. UV/vis spectra, recorded after photolysis ($\lambda > 320$ nm, 3 min) of **1** in CH_3CN . The top four spectra were recorded with a spacing of 30 s. The spectrum showing the lowest absorption at $\lambda = 470$ nm represents the end point (after 15 min). Inset: Plot of $\ln A$ (470 nm) vs time (in seconds), and linear fit to $\ln A$ vs t (s).

with acrylonitrile was calculated by density functional theory²⁰ as $\Delta H^\ddagger = 29.5 \text{ kcal mol}^{-1}$. This relatively high value explains the lack of reactivity toward acrylonitrile.²¹ The long lifetime of **9**, coupled with high reactivity toward water, is consistent with the efficient formation of **4**, even under almost anhydrous conditions. The residual absorption with λ_{max} around 370 nm can be attributed to the aminobenzaldehyde **4** (see Experimental section).

Low-Temperature Spectroscopy. Cryptand **1** and the complexes NaBr@1 and KBr@1 were photolyzed at 77 K in 2-methyltetrahydrofuran (MTHF), ethanol, or a 5:5:2 mixture of diethyl ether, isopentane, and ethanol (EPA mixture). The photochemistry was investigated using EPR spectroscopy. EPR spectra obtained after photolysis of **1** (in glassy ethanol or MTHF glass (see Figure 2)) and NaBr@1 or KBr@1 (in glassy ethanol or in MTHF) at 77 K showed transitions at 6680 G (**1**, in MTHF), 6720 G (**1**, in EtOH), 6560 G (NaBr@1 , in EtOH), and 6597 G (KBr@1 , in MTHF). These transitions are typical of triplet aryl nitrenes^{22a} and can thus be assigned to triplet **2**, triplet NaBr@2 , and triplet KBr@2 . From the spectra, zero-field splitting (ZFS) parameters can be derived as $D' = 0.93 \text{ cm}^{-1}$ (**2**, in EtOH), $D' = 0.92 \text{ cm}^{-1}$ (**2**, in MTHF), $D' = 0.88 \text{ cm}^{-1}$ (NaBr@2 , in EtOH), and $D' = 0.89 \text{ cm}^{-1}$ (KBr@1 , in MTHF). The similarity of the EPR spectra of $^3\mathbf{2}$, $\text{NaBr@}^3\mathbf{2}$, and $\text{KBr@}^3\mathbf{2}$ indicates that complexation with Na^+ or K^+ does

(20) B3LYP/6-31G(d).

(21) *exo*-Attack, formation of the 2-cyanotetrahydroquinoline derivative. Simpler iminoquinone methides, as described in ref 14, are considerably more reactive toward dienophiles. The reason for the significantly reduced reactivity of *Z*-**9** is unclear at present. Most likely, steric factors play a role.

(22) (a) Smolinsky, G.; Wasserman, E.; Yager, Y. A. *J. Am. Chem. Soc.* **1962**, *84*, 3220. (b) The signals at ~ 3400 G are narrow triplets, which are assigned to aminyl/alkyl radical pairs formed by intramolecular hydrogen abstraction by the nitrene from a crown ether methylene group.

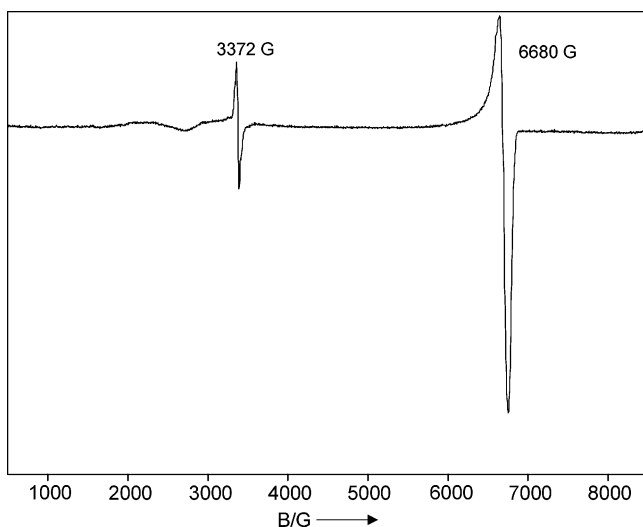


Figure 2. Triplet EPR spectrum obtained upon photolysis ($\lambda = 254$ nm, 5 min) of **1** in glassy MTHF at 4 K.

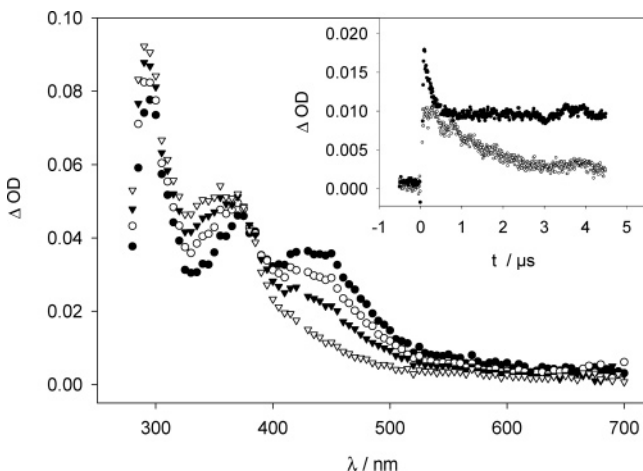


Figure 3. Transient spectra detected after LFP (266 nm) of azido-cryptand **1** in CH_3CN . Black circles: time window 0.4–0.54 μs after LFP; white circles: 0.73–0.95 μs ; black triangles: 1.21–1.41 μs ; white triangles: 2.76–3.25 μs . Inset: transient traces. White: observed at $\lambda = 445$ nm following LFP of **1**. Black: observed at $\lambda = 440$ nm following LFP of NaBr@1 .

not lead to a dramatic change of the electronic properties of 32 . Only small changes are observed in the position of the transition at ca. 6600–6700 G and in the fine structure of the bands at ca. 3400 G.^{22b}

Laser Flash Photolysis. The photochemistry of **1**, NaBr@1 , and KBr@1 was investigated by nanosecond time-resolved laser flash photolysis (LFP). LFP ($\lambda_{\text{exc}} = 266$ nm, acetonitrile, ambient temperature, 1 atm Ar) of **1** gave the transient spectrum shown in Figure 3. Transients were detected with $\lambda_{\text{max}} = 295$ and ca. 370 nm (first-order growth, $\tau = 1.4$ μs , followed by decay, $\tau \approx 8$ ms (transient **B**²³)) and $\lambda_{\text{max}} = 445$ nm (first-order decay, $\tau = 1.4$ μs , transient **A**). Additionally, a broad and very weak transient absorption was detected at $\lambda > 500$ nm (first-order decay, $\tau \approx 1.4$ μs , transient **A**). The observations thus yield a mechanistic scenario, $\mathbf{1} \rightarrow \mathbf{A} \rightarrow \mathbf{B}$, the lifetimes being $\tau = 1.4$ μs for **A** and 8 ms for **B**. Transient **B** is quenched

(23) Before assignment, the set of reactive intermediates generated by laser flash photolysis will be labeled with capital letters **A**, **A'**, **A''**, **B**, **B'**, **B''**, **C**, **C''**, **D'**, **E''**. Unprimed letters refer to the uncomplexed ligands, ' indicates complexation to Na^+ , while '' indicates complexation to K^+ .

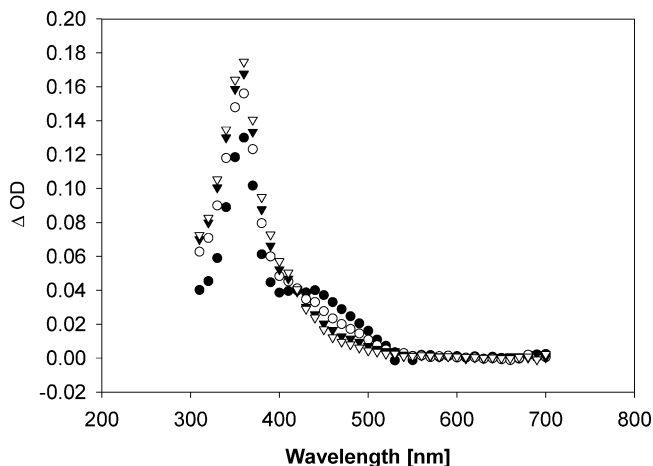


Figure 4. Transient spectra, observed during different time windows after LFP (266 nm) of NaBr@1 in acetonitrile under 1 atm Ar. Black circles: 320–360 ns, white circles: 410–460 ns, black triangles: 540–620 ns, white triangles: 1.63–1.80 μs after the laser pulse.

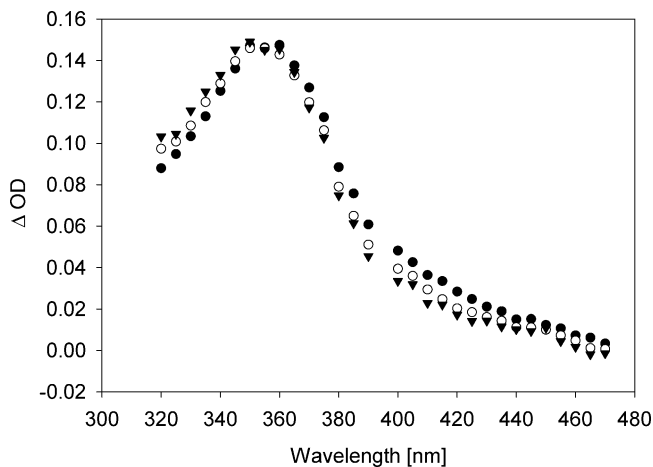


Figure 5. Transient spectra, observed during different time windows after LFP (266 nm) of KBr@1 in acetonitrile under 1 atm Ar. Black circles: 11–52 μs , white circles: 340–400 μs , black triangles: 1.4–1.6 ms after the laser pulse.

by diethylamine. Plotting the decay rate constant of **B** vs $[\text{HNEt}_2]$ yields the rate constant for the reaction of **B** with diethylamine as $k_{\text{HNEt}_2} = (5.4 \pm 0.5) \times 10^3 \text{ L mol}^{-1} \text{ s}^{-1}$ (see Supporting Information, Figure S1).

LFP of NaBr@1 and KBr@1 resulted in the formation of transient species showing similar spectra and lifetimes. In the following section, we will place our focus on the photochemistry of the potassium complex KBr@1 , mentioning differences from the sodium complex if applicable.

Upon LFP ($\lambda_{\text{exc}} = 266$ nm, acetonitrile, Ar atmosphere) of KBr@1 , we detected transients **A''** with $\lambda_{\text{max}} \approx 460$ nm (first-order decay, $\tau = 160$ ns (Na complex: transient **A'**, $\tau = 200$ ns)) and a transient **B''** with $\lambda_{\text{max}} = 295, 350$ nm (first-order growth, $\tau = 160$ ns, no decay on a time scale up to 20 ms). Figure 4 shows transient spectra recorded during different time intervals shortly after LFP (266 nm) of NaBr@1 , while Figure 5 shows the spectral characteristics of the longer-lived transients observed after LFP of KBr@1 in acetonitrile. In both time regimes, the transient spectra recorded after LFP of NaBr@1 and KBr@1 look virtually identical.

Additionally, a transient **C''** was observed (Figure 5: first-order growth, $\tau = 160$ ns, followed by first-order decay, $\tau =$

Table 1. Summary of Experimental Results Obtained by LFP of **1**, NaBr@**1**, and KBr@**1**

precursor	trans.	λ_{\max} [nm]	lifetime τ	properties	assignment
1	A	445	decay: 1.4 μ s	decays to B quenched by HNEt ₂ $k_q = (5.4 \pm 0.5) \times 10^3 \text{ L mol}^{-1} \text{ s}^{-1}$ decays to B' and C'	12
1	B	295, 370	growth: 1.4 μ s decay: 8 ms		7
NaBr@ 1	A'	460	decay: 200 ns	decays to B'' and C'' quenched by HNEt ₂ $k_q = (3.0 + 0.8) \times 10^6 \text{ L mol}^{-1} \text{ s}^{-1}$ quenched by HNEt ₂ to yield E'' $k_q \approx 2 \times 10^7 \text{ L mol}^{-1} \text{ s}^{-1}$ decays to D''	NaBr@ 12
NaBr@ 1	B'	295, 350	growth: 200 ns no decay on ms time scale		NaBr@ 7
NaBr@ 1	C'	400	growth: 200 ns decay: 250 μ s		NaBr@ 16
KBr@ 1	A''	460	decay: 160 ns	decays to B'' and C'' quenched by HNEt ₂ $k_q = (3.0 + 0.8) \times 10^6 \text{ L mol}^{-1} \text{ s}^{-1}$ quenched by HNEt ₂ to yield E'' $k_q \approx 2 \times 10^7 \text{ L mol}^{-1} \text{ s}^{-1}$ decays to D''	KBr@ 12
KBr@ 1	B''	295, 350	growth: 160 ns no decay on ms time scale		KBr@ 7
KBr@ 1	C''	400	growth: 160 ns decay: 310 μ s		KBr@ 16
KBr@ 1	D''	320	growth: 300 μ s no decay on ms time scale		KBr@ 8
KBr@ 1	E''	350 ^a	decay: 1 ms		formed only in the presence of HNEt ₂

^a Absorption maximum not determined, shows absorption at $\lambda = 350 \text{ nm}$.

310 μ s, $\lambda_{\max} = 400 \text{ nm}$ (Na complex: transient **C'**, $\tau_{\text{decay}} = 250 \mu\text{s}$). Concomitant with the decay of transient **C''**, we observed the growth of a product **D''** ($\tau_{\text{growth}} \approx 300 \mu\text{s}$, stable up to 20 ms, $\lambda_{\max} \leq 320 \text{ nm}$, Figure 5) The mechanistic scenario thus ensues as $\text{KBr@1} \rightarrow \text{A''} \rightarrow \text{B''} + \text{C''}$ and $\text{C''} \rightarrow \text{D''}$.

Addition of diethylamine results in a shortening of the lifetime of **A''** ($k_{\text{HNEt}_2} = (3.0 \pm 0.8) \times 10^6 \text{ L mol}^{-1} \text{ s}^{-1}$, see Figure S2) and of **B''** ($k_{\text{HNEt}_2} \approx 2 \times 10^7 \text{ L mol}^{-1} \text{ s}^{-1}$). In the presence of diethylamine, a second long-lived decaying transient, **E''**, is monitored at $\lambda = 350 \text{ nm}$ ($\tau \approx 1 \text{ ms}$, τ independent of [HNEt₂]). It is noted that the evaluation of the transient traces of **B''** and **E''** ($\lambda = 350 \text{ nm}$) in the presence of diethylamine is made difficult by the biexponential decay kinetics. For that reason, only an approximate value for the rate constant of the **B''** + HNEt₂ reaction is given.

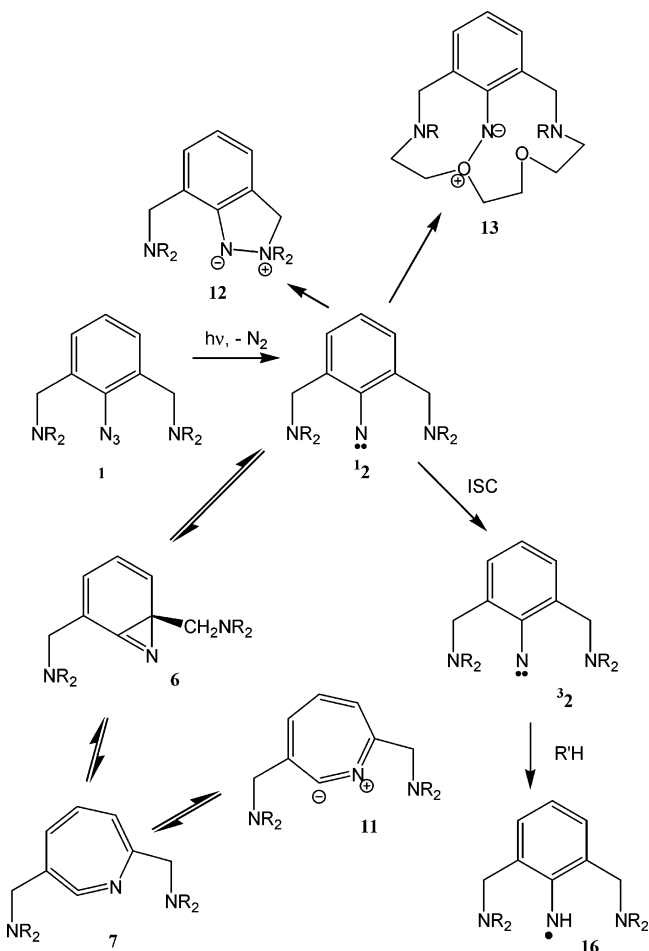
To facilitate the discussion, the results obtained by LFP are summarized in Table 1. The assignment of the transients will be rationalized in the following section.

In the following section, the transients observed will be assigned to chemical structures. To achieve the assignments, we have employed density functional as well as MCSCF ab initio MO theory.

Assignment of Transients, Calculations, and Discussion

Identification of Transients B, B', and B''. Among the transients observed, the assignment of **B** appears to be the most straightforward. Here, the characteristic UV/vis spectrum as well as the typical reactivity toward diethylamine points to didehydroazepine **7**. Due to the similar spectral characteristics and lifetimes, **B'** and **B''** are assigned to the complexed didehydroazepines NaBr@**7** (**B'**) and KBr@**7** (**B''**). Complexation to Na⁺ or K⁺ should make **7** more electrophilic and thus increase its reactivity toward diethylamine. This is also observed experimentally.

Identification of Transients A, A', and A''. The short-lived transients **A**, **A'**, and **A''** are precursors to the transients **B**, **B'**, and **B''**, which have been identified as didehydroazepines **7**, NaBr@**7**, and KBr@**7**. Transient species that could potentially play that role are shown in Scheme 4: singlet nitrenes **12** (**A**), NaBr@**12** (**A'**), and KBr@**12** (**A''**), or triplet nitrenes **32** (**A**),

Scheme 4. Possible Reaction Pathways Following Excitation of **1**^a

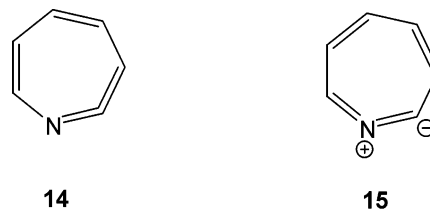
^a NR₂...NR₂ indicates bridging by diaza-18-crown-6. In the case of **13**, one of the two crown ether bridges is shown explicitly.

NaBr@**32** (**A'**), and KBr@**32** (**A''**), azirines **6** (**A**), NaBr@**6** (**A'**), and KBr@**6** (**A''**), or the cyclic nitride ylides **11**, NaBr@**11**, and KBr@**11**. Other possibilities include the amine ylide **12** or the ether ylide **13** and their complexes. Both **12** and **13** could in principle play the role of masked singlet nitrenes, which could convert to the didehydroazepines at the relatively slow rates observed experimentally.

DFT calculations were performed in order to identify the species observed. Trends in differences in energy between given triplet aryl nitrenes and the corresponding didehydroazepines should be predictable with reasonable accuracy by density functional theory (B3LYP/6-31G(d)). The energy differences between **32** and **7**, Na⁺@**32** and Na⁺@**7**, and K⁺@**32** and K⁺@**7** thus calculated are $\Delta H = 8.4 \text{ kcal mol}^{-1}$ (uncomplexed), $14.8 \text{ kcal mol}^{-1}$ (Na complex), and $14.2 \text{ kcal mol}^{-1}$ (K complex), in favor of the triplet nitrenes. These results essentially rule out a possible assignment of **A**, **A'**, and **A''** as **32**, NaBr@**32**, and KBr@**32**. A triplet nitrene that is lower in energy by 8–15 kcal/mol than the corresponding didehydroazepine will not decay to this didehydroazepine on a nanosecond time scale.^{24a} It is noted that these results agree well with the results of previous computational studies on simpler aryl nitrenes, where the triplet nitrenes were consistently found to be lower in energy than the didehydroazepines.^{24b–27}

Transient **A** shows an absorption maximum at $\lambda = 445 \text{ nm}$ plus a very weak long-wavelength absorption at $\lambda > 500 \text{ nm}$. An absorption at this wavelength would be atypical for bridged azirines **6**.^{28–30,31a} We calculated the activation and reaction enthalpies for the electrocyclic ring-opening reactions **6** → **7**, Na⁺@**6** → Na⁺@**7**, and K⁺@**6** → K⁺@**7**. At the B3LYP/6-31G(d) level of theory, the results were $\Delta H^\ddagger = 3.5 \text{ kcal/mol}$ and $\Delta H = -5.9 \text{ kcal/mol}$ (**6** → **7**), $\Delta H^\ddagger = 3.6 \text{ kcal/mol}$ and $\Delta H = -9.7 \text{ kcal/mol}$ (Na⁺@**6** → Na⁺@**7**), and $\Delta H^\ddagger = 4.4 \text{ kcal/mol}$ and $\Delta H = -6.6 \text{ kcal/mol}$ (K⁺@**6** → K⁺@**7**). The calculations thus predict that K⁺@**6** should undergo ring-opening more slowly than **6**, which is in contrast to the experimentally determined behavior of transients **A** and **A''** (**A''** decaying faster than **A** by a factor of 9). Hence, an assignment of **A**, **A'**, and **A''** to the bicyclic azirines **6**, NaBr@**6**, and KBr@**6** can be ruled out. Cyclic nitrile ylides related to **11** and its complexes have recently been characterized as products formed in the course of photolysis of both 1-naphthyl- and 2-naphthyl azide in an argon matrix.^{31a} These benzo-annelated derivatives of **15** show UV/vis absorption maxima (λ_{max} around 450 nm) that would agree well with the experimental data for **A**, **A'**, and **A''**. Nevertheless, their formation upon photolysis of **1**, NaBr@**1**, or KBr@**1** appears unlikely. According to Karney and Borden,²⁶ didehydroazepine **14** is calculated (CASPT2N/6-31G*//CASSCF(8,8)/6-31G*) to be lower in energy than its bond-shift isomer **15** by 25 kcal/mol. There is no obvious reason why the relative energies of **7** and **11** should

differ significantly from this figure. The cyclic nitrile ylide **11** can thus be estimated to be higher in energy than singlet nitrene **12** by ca. 23 kcal/mol, which rules out its formation under conditions of laser flash photolysis.^{31b}



The amine ylide **12** and the ether ylide **13** and their complexes were also considered as possible intermediates. In a related system, we were recently able to obtain indirect evidence for the formation of a nitrene-amine ylide.³² Very little evidence for nitrene-ether ylides has been reported so far,³³ while more data have been presented for carbene-ether ylides.³⁴ The formation of these two species from the S₁ state of the nitrene might involve a conical intersection connecting the open-shell nitrene and closed-shell ylide surfaces.³⁵ As far as **12** and its complexes are concerned, it appears highly unlikely that they should play the role of masked singlet nitrenes for two reasons. First, no evidence was obtained for the product expected for such a reaction, which would be an indazole derivative.³² Second, DFT (B3LYP/6-31G(d)) predicts the uncomplexed ylide **12** to be lower in energy than didehydroazepine **7** by 21.6 kcal/mol, which rules out a thermal rearrangement **12** → **7** and thus excludes the involvement of **12** in the process. The formation of ether ylide **13**, on the other hand, is predicted to be too unfavorable for **13** to play a role in the process. On the B3LYP/6-31G(d) level of theory, **13** is predicted to be higher in energy than didehydroazepine **7** by 34.2 kcal/mol. Under the assumption that nitrene **12** and **7** do not strongly differ in energy, **13** is much higher in energy than **12** and should therefore not be formed.^{36a} Moreover, it appears highly unlikely that an ether ylide should be formed in the case of the alkali metal complexes, where the nucleophilicity of the ether oxygen atoms is greatly reduced due to complexation to the metal cations.^{36b}

The singlet aryl nitrenes **12**, NaBr@**12**, and KBr@**12** remain as sole candidates for an assignment of **A**, **A'**, and **A''**. If this assignment is to hold, an explanation for the unusually long lifetimes of **12**, NaBr@**12**, and KBr@**12** is required. Singlet aryl nitrenes usually decay both by ring-closure to bicyclic azirines (in our system: **6** and its complexes) and by ISC to the ground state triplet nitrenes (here: **32**, NaBr@**32**, and KBr@**32**).

A look at the calculated geometry of singlet nitrene **12** (Figure 6) could offer an explanation for a very slow rate of ring-closure to **6**. This reaction should be impeded by the presence of the methylenic protons in the *ortho* substituents. Unlike in singlet 2,6-dimethyl phenylnitrene, the *ortho* substituents in **12** cannot easily be rotated in order to better accommodate the nitrene

- (24) (a) Using the same method, the cyclization of parent triplet phenylnitrene to didehydroazepine is calculated to be endothermic by 14.8 kcal/mol. Hence, the complexed cryptand systems behave “normally”, while the uncomplexed cryptand nitrene **32** must be destabilized by the electron-rich environment, or else the didehydroazepine **7** stabilized, or both. (b) Hrovat, D. A.; Waali, E. E.; Borden, W. T. *J. Am. Chem. Soc.* **1992**, *114*, 8698.
 (25) Kim, S.-J.; Hamilton, T. P.; Schaefer, H. F., III. *J. Am. Chem. Soc.* **1992**, *114*, 5349.
 (26) Karney, W. L.; Borden, W. T. *J. Am. Chem. Soc.* **1997**, *119*, 1378.
 (27) Gritsan, N. P.; Zhu, Z.; Hadad, C. M.; Platz, M. S. *J. Am. Chem. Soc.* **1999**, *121*, 1202.
 (28) Morawietz, J.; Sander, W. *J. Org. Chem.* **1996**, *61*, 4351.
 (29) Tsao, M.-L.; Gritsan, N.; James, T. R.; Platz, M. S.; Hrovat, D. A.; Borden, W. T. *J. Am. Chem. Soc.* **2003**, *125*, 9343.
 (30) Tsao, M.-L.; Platz, M. S. *J. Am. Chem. Soc.* **2003**, *125*, 12014.
 (31) (a) Maltsev, A.; Bally, T.; Tsao, M.-L.; Platz, M. S.; Kuhn, A.; Vosswinkel, M.; Wentrup, C. *J. Am. Chem. Soc.* **2004**, *126*, 237. (b) The cyclic nitrile ylides described in ref 28a owe their stability to the destabilization of the corresponding *ortho*-quinoid didehydroazepines. This factor does not apply to **7/11** or **14/15**. In the parent system, didehydroazepine **14** is calculated (ref 26) to be lower in energy than singlet phenylnitrene (¹A₂) by 1.6 kcal/mol. From the 25 kcal/mol difference in energy between **14** and **15** and this, the difference in energy between **12** and **11** can thus be estimated as 23 kcal/mol.

- (32) Tönshoff, C.; Bucher, G. *Eur. J. Org. Chem.* **2004**, 269.
 (33) Poe, R.; Schnapp, K.; Young, M. J. T.; Grayzar, J.; Platz, M. S. *J. Am. Chem. Soc.* **1992**, *114*, 5054.
 (34) (a) Naito, I.; Oku, A.; Otani, N.; Fujiwara, Y.; Tanimoto, Y. *J. Chem. Soc., Perkin Trans. 2* **1996**, 725. (b) Wang, J.-L.; Yuzawa, T.; Nigam, M.; Likhovorik, I.; Platz, M. S. *J. Phys. Chem. A* **2001**, *105*, 3752.
 (35) Bucher, G.; Nicolaidis, A., unpublished results.
 (36) (a) We cannot rule out formation of **13** from higher excited singlet states of either **1** or **2**. (b) All attempts at optimizing the structure of **13** complexed to Na⁺ resulted in cleavage of the N–O bond and convergence to a nitrene structure.

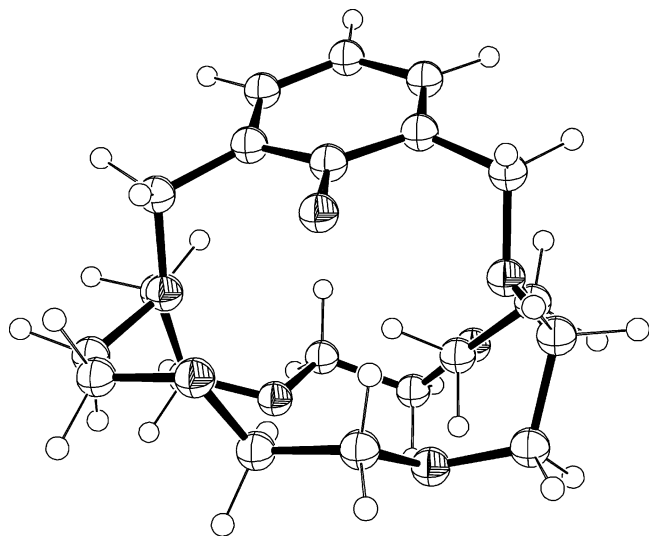


Figure 6. ORTEP drawing of the calculated geometry (MCSCF(8,8)/STO-3G) of singlet nitrene **12**.

nitrogen approaching the *ortho* carbon. According to Borden and Karney, freezing the orientation of the *ortho* methyl groups in singlet 2,6-dimethyl phenylnitrene leads to a barrier that is higher by ca. 1 kcal/mol.³⁷ An increment in barrier height of this size is compatible with the observed slow kinetics of the decay of **12**.

The influence of a cryptand structure on the ISC rate constant of singlet aryl nitrenes is much more difficult to assess. In a recent publication,³⁸ Cramer and co-workers have tried to rationalize the substituent effect on ISC of phenylnitrenes. According to their model, the ISC rate depends on the contribution of the configuration of the S_3 singlet to the wave function describing the S_1 singlet, but not on the contribution of the S_2 singlet. This S_3 contribution was approximated empirically and was shown to reproduce qualitatively the trends of the experimental observations. Furthermore, there are two aspects to this contribution. First, S_1 – S_3 mixing should correlate with the energy difference between the two states (the smaller the energy difference, the larger the mixing). This is a thermodynamic factor. As it is conceivable that in the cryptand system the unusual environment of the nitrene center may affect this energy difference, we calculated at the MCSCF(8,8)/STO-3G level of theory the energies of the S_2 and S_3 electronic states of singlet nitrene **12** and $\text{Na}^+@2$ at the optimum geometry of the lowest singlet (S_1). For comparison, the same level of theory was used to compute the energies of the S_2 and S_3 excited singlets of phenylnitrene at the optimum geometry of its S_1 state.

Our multireference computations find the S_1 – T_0 splitting in **2** to be 27.0 kcal/mol, and 24.9 kcal/mol for $\text{Na}^+@2$. This is rather similar to the S_1 – T_0 splitting of phenylnitrene (28.9 kcal/mol) at the same level of theory. At the optimum geometry of state S_1 , the S_2 state of **2** is computed to lie 44.5 kcal/mol higher than S_1 (40.3 and 37.4 kcal/mol in the cases of $\text{Na}^+@2$ and phenylnitrene, respectively), while (at the same geometry) the S_3 state of **2** is calculated to be 61.3 kcal/mol higher than S_1 (61.5 and 62.2 kcal/mol in the cases of $\text{Na}^+@2$ and phenylnitrene, respectively). Thus, although the cryptand seems to affect

the relative energy of the S_2 state, it has little if any effect on the relative energy of the S_3 state. Correspondingly, a change in the ISC rate cannot be related to the relative energies of the S_3 states.

Second, the mixing of S_1 and S_3 may be influenced by dynamic factors. In this respect, the pronounced retardation of ring expansion in **12** might offer a clue for the slow rate of ISC observed. We quote from the work of Cramer and co-workers:³⁸ “Bulky *ortho* groups should serve not merely to decrease rates of ring expansion, but also to decrease fluxionality in the system as a whole. In that case, dynamical mixing of S_1 and S_3 may well be decreased, and strong donors at the *para* position should then be able to play a favorable role in further increasing the activation enthalpy for ring expansion without playing a negative role by contributing to higher rates of ISC.” In the case of **12**, the difficulty in proceeding along the reaction coordinate connecting S_1 and azirine **6** would thus also reduce the dynamical mixing of S_1 and S_3 . This should lead to a decrease in ISC rate constant.

The absorption maximum of **12**, $\lambda_{\text{max}} = 445$ nm, is somewhat unusual, as most singlet aryl nitrenes observed so far show strong absorption bands only at shorter wavelengths ($\lambda_{\text{max}} = 350$ nm for singlet PhN).^{4,5} However, certain derivatives of singlet phenylnitrene have been reported to show absorption maxima around $\lambda = 470$ nm, such as the singlet nitrene derived from *N*-propyl-4-azido-2,3,5,6-tetrafluorobenzamide.^{39a} TD-DFT calculations on **12** also yield evidence for absorption between 400 and 500 nm.^{39b}

Assignment of Transients C' and C''. In the context of an assignment of **A**, **A'**, and **A''** as **12**, $\text{NaBr}@12$, and $\text{KBr}@12$, the observation of a faster decay of the complexed transient could possibly be rationalized in terms of an internal heavy atom effect of the sodium and potassium cations, which would accelerate intersystem crossing. From this, an assignment of **C'** and **C''** as $\text{NaBr}@32$ and $\text{KBr}@32$ would follow. Spin–orbit coupling (SOC) resulting from the presence of the heavy alkali metal cations should also manifest itself in the ESR spectra of the ground state triplet nitrenes, where it should lead to an increase in the ZFS parameter D .⁴⁰ The effect of alkali cation complexation on the ZFS parameters of the triplet nitrenes, however, is small, and opposite of what is required ($D' = 0.93$ cm^{-1} (**32**, in EtOH); $D' = 0.88$ cm^{-1} ($\text{NaBr}@32$, in EtOH)). For that reason, an assignment of **C'** and **C''** to the triplet nitrenes **32** and $\text{NaBr}@32$ does not appear to be correct.

More likely, **C'** and **C''** can be assigned to the aminyl radicals **16** formed from the singlet nitrenes by hydrogen abstraction (Scheme 5). The phenylaminyl radical has been reported to show a $\lambda_{\text{max}} = 400$ nm,⁴¹ which would agree well with the transient absorption measured in our experiments. As the ether bridges present in the cryptand system represent good hydrogen donors, it is also conceivable that hydrogen abstraction takes place from one of them, although the presence of alkali cations should make this somewhat more difficult. We note that the quenching of **A''** with diethylamine observed in the LFP experiments and the isolation of the product (i.e., the aniline **8**) derived from this

(37) Karney, W. L.; Borden, W. T. *J. Am. Chem. Soc.* **1997**, *119*, 3347.

(38) Johnson, W. T. G.; Sullivan, M. B.; Cramer, C. J. *Int. J. Quantum Chem.* **2001**, *85*, 492.

(39) (a) Pol'shakov, D. A.; Tsentalovich, Yu. P.; Gritsan, N. P. *Kinet. Catal.* **2001**, *42*, 601; *Kinetika Kataliz* **2001**, *42*, 664. (b) For **12**, TD-UB3LYP/6-31+G*/MCSCF(8,8)/STO-3G predicts moderately intense absorptions at $\lambda_{\text{max}} = 511$, 447, and 411 nm.

(40) Havlas, Z.; Kývala, M.; Michl, J. *Collect. Czech. Chem. Commun.* **2003**, *68*, 2335.

(41) Leyva, E.; Platz, M. S.; Niu, B.; Wirz, J. *J. Phys. Chem.* **1987**, *91*, 2293.

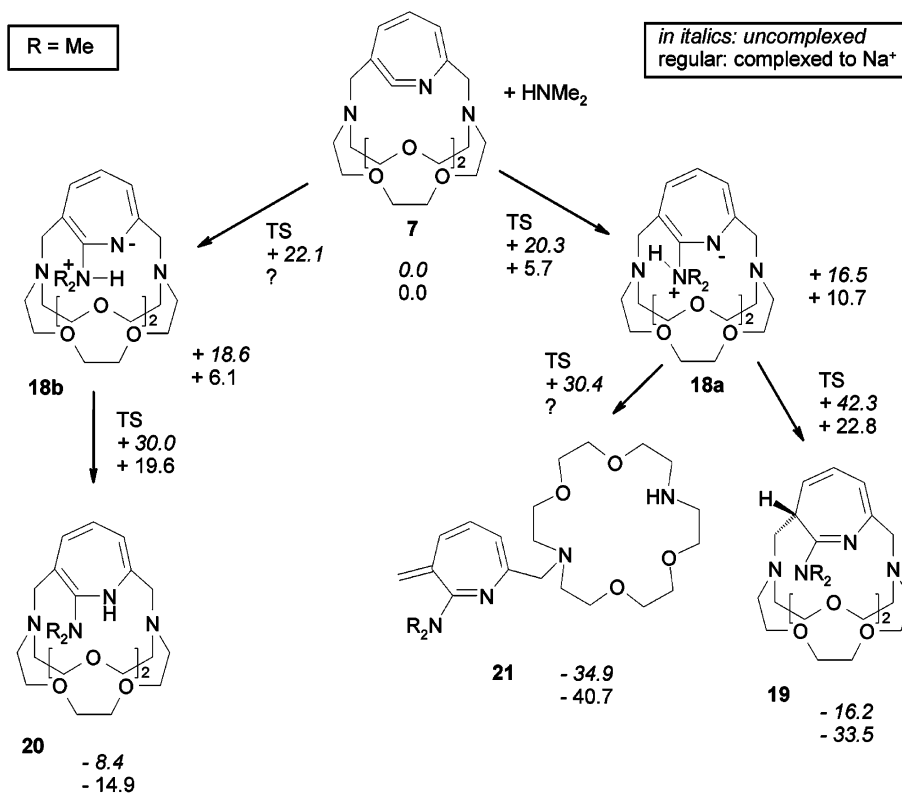
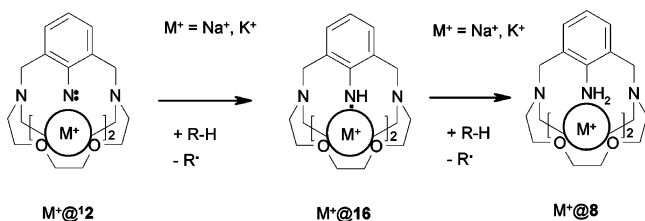


Figure 7. Energies (in kcal/mol, relative to the precursors) of stationary points along the reaction coordinates of the reactions of **7** (in italics) and Na^+ @**7** (regular font) with dimethylamine, as calculated at the ipcm-B3LYP/6-31G(d)//B3LYP/6-31G(d) + ZPE level of theory. In the ipcm calculations, acetonitrile was the solvent specified.

Scheme 5

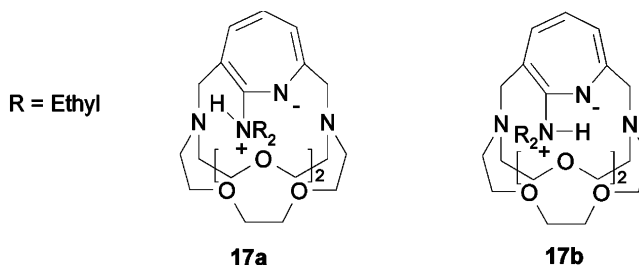


hydrogen abstraction reaction argue in favor of an assignment of **C'** and **C''** as aminyl radicals NaBr@16 and KBr@16 . A rate constant of $k = (3.0 \pm 0.8) \times 10^6 \text{ L mol}^{-1}$ for the reaction of **A''** with diethylamine is in the range expected for reactions of moderately reactive diradicals with good hydrogen donors.⁴²

Assignment of Transients/Products D'' and E''. Product **D''** is formed concomitant with the decay of **C''**. For that reason, it appears likely that **D''** corresponds to a stable product derived from aminyl radical **16**, such as the potassium complex of aniline **8**.

Transient **E''** is observed in the presence of diethylamine as added quencher. Its lifetime ($\tau \approx 1 \text{ ms}$ in acetonitrile) does not depend on the concentration of diethylamine. At present, we can only speculate about its nature. It appears conceivable that **E''** could correspond to the zwitterionic primary adduct **17** of

the potassium complex of didehydroazepine **7** and diethylamine. Zwitterion **17** may exist as two rotamers, **17a** and **17b**.



Reaction of 7 and Its Sodium Complex with Secondary Amines. To obtain further evidence for the formation of alkali metal complexes of **17**, we performed DFT calculations on the reaction of **7** as well as Na^+ @**7** with dimethylamine as model substrate. Geometries were optimized at the B3LYP/6-31G(d) level of theory. Solvation by acetonitrile was taken into account by performing ipcm single-point calculations at the same level of theory.⁴³ The data are corrected for ZPE. The results are shown in Figure 7.

The calculations indicate that the addition of secondary amines should be much faster for the complexed didehydroazepines than for the uncomplexed one, as is also observed experimentally. Moreover, they show that in the case of the uncomplexed didehydroazepine, the primary addition yielding the zwitterionic intermediate should be the rate-determining step, while in the case of the complexed didehydroazepines, the follow-up reactions are predicted to be slower than the initial

(42) For example, the rate constant for the reaction of triplet diphenylcarbene with triethylamine has been determined as $k = (3.4 \pm 1.4) \times 10^3 \text{ M}^{-1} \text{ s}^{-1}$ (Hadel, L. M.; Platz, M. S.; Scaiano, J. C. *J. Am. Chem. Soc.* **1984**, *106*, 283.) It is noted that the reactions of fluorinated singlet aryl nitrenes with secondary amines have been reported to yield hydrazine derivatives as main products (ref 33). These were not observed in our system. The quenching of NaBr@12 or KBr@12 by diethylamine also partially accounts for our failure to isolate **5** upon photolysis of complexes of **1** in the presence of diethylamine (Stern–Volmer quenching). In addition, complexes of **5** may also simply be too unstable for isolation (cf. ref 17 and references therein).

(43) Foresman, J. B.; Keith, T. A.; Wiberg, K. B.; Snoonian, J.; Frisch, M. J. *J. Phys. Chem.* **1996**, *100*, 16098.

addition of dimethylamine. This is consistent with the observation of only one transient, didehydroazepine **7**, upon LFP of **1** in the presence of diethylamine, while a second, longer-lived transient **E''** (likely a potassium complex of the diethylamino-substituted zwitterion **17b**) was additionally observed upon LFP of **KBr@1**. According to our calculations, the most favorable reaction pathway for the reaction of **7** with dimethylamine runs via zwitterion **18a**, followed by proton transfer to the tertiary amine concerted with cleavage of the benzylic C–N bond, yielding methyleneazepine **21**. We note that the barriers calculated are too high to be consistent with a rate constant of $k = 5.4 \times 10^3 \text{ L mol}^{-1} \text{ s}^{-1}$ for the reaction of **7** with diethylamine. This, however, may only reflect the need to further refine the computational methodology, and to optimize the geometries of solvated stationary points (in particular the polar zwitterions) using a scrf method. In the case of the reaction of the sodium complex $\text{Na}^+@7$ with dimethylamine, we have not been able to locate a transition state for the formation of $\text{Na}^+@18b$. At least in the gas phase, this reaction thus likely proceeds with little or no barrier.

Conclusion

Complexation to alkali cations has a considerable impact on nitrene chemistry. The influence on singlet nitrene chemistry is most pronounced. The binding of Na^+ or K^+ leads not only to a significant decrease in lifetime but also to a much increased reactivity in intermolecular reactions. For example, hydrogen abstraction is a reaction pathway that is only observed in case of the complexed singlet nitrenes. On the side of the triplet nitrenes, only a small effect was found on the ZFS parameters, and this small effect is not indicative of increased spin–orbit coupling (heavy-atom effect). The reactivity of didehydroazepines toward diethylamine is significantly increased by complexation, which is understandable in terms of increased

electrophilicity induced by the cationic guest. Our experiments indicate that the complexed didehydroazepines $\text{NaBr}@7$ and $\text{KBr}@7$ are longer lived rather than shorter lived, as compared to the uncomplexed species **7**. This might be taken as indication that other decay channels available to didehydroazepines, such as reversible ring-contraction and -opening yielding the singlet nitrene followed by ISC to the ground state triplet nitrene or polymerization, do not necessarily have to be made faster by complexation.

The cryptand environment itself has a profound influence on the reactivity of the reactive species investigated. The rigidity of the molecular framework prevents rapid cyclization of the singlet nitrenes to bridged azirines and didehydroazepines, as it is otherwise observed for aryl nitrenes. Recent theoretical work³⁸ suggests that the same factor also disfavors ISC to the ground state triplet nitrenes. For this reason, a record lifetime of $\tau = 1.4 \mu\text{s}$ is measured for the uncomplexed singlet cryptand nitrene **12**. Singlet nitrene **12** in part undergoes 1,4-hydrogen transfer to yield iminoquinone methide **9**, which itself is remarkably long-lived with a lifetime τ of more than 4 min in acetonitrile solution at ambient temperature.

Acknowledgment. Financial support by the Deutsche Forschungsgemeinschaft (SFB 452) and the Dr. Otto Röhm–Gedächtnisstiftung is gratefully acknowledged. G.B. thanks W. T. Borden and R. J. McMahon for helpful discussions. We thank H.-H. Wenk and K. Gomann for their help with the EPR measurements.

Supporting Information Available: Figure S1: Plot of the rate constant of decay of transient **B** vs. the concentration of diethylamine. Figure S2: Plot of the rate constant of decay of transient **A''** vs. the concentration of diethylamine. This material is available free of charge via the Internet at <http://pubs.acs.org>.

JA0447208